Environmental Microbiology
May 2021, Volume 23 Issue 5 Pages 2592-2604
https://doi.org/10.1111/1462-2920.15482
https://archimer.ifremer.fr/doc/00909/102091/

Seasonal marine microorganisms change neighbours under contrasting environmental conditions

Lambert Stefan [1], Lozano Jean-claude [1], Bouget François-yves [1, *], Galand Pierre E. [2, *]

[1] Sorbonne Université, CNRS, Laboratoire d'Océanographie Microbienne (LOMIC), Observatoire Océanologique de Banyuls Banyuls sur Mer ,France
[2] Sorbonne Université, CNRS, Laboratoire d'Ecogéochimie des Environnements Benthiques (LECOB), Observatoire Océanologique de Banyuls Banyuls sur Mer, France

* Corresponding authors : François-Yves Bouget, email address : francois-yves.bouget@obs-banyuls.fr ; Pierre E. Galand, email address : pierre.galand@obs-banyuls.fr

Abstract :

Summary Marine picoplankton contribute to global carbon sequestration and nutrient recycling. These processes are directly related to the composition of communities, which in turn depends on microbial interactions and environmental forcing. Under regular seasonal cycles, marine communities show strong predictable patterns of annual re-occurrences, but little is known about the effect of environmental perturbation on their organization. The aim of our study was to investigate the co-occurrence patterns of planktonic picoeukaryote, bacteria and archaea under contrasting environmental conditions. The study was designed to have high sampling frequency that could match both the biological rhythm of marine microbes and the short time scale of extreme weather events. Our results show that microbial networks changed from year to year depending on conditions. In addition, individual taxa became less interconnected and changed neighbours, which revealed an unfaithful relationship between marine microorganisms. This unexpected pattern suggests possible switches between organisms that have similar specific functions, or hints at the presence of organisms that share similar environmental niches without interacting. Despite the observed annual changes, the time series showed re-occurring communities that appear to recover from perturbations. Changing co-occurrence patterns between marine microorganisms may allow the long-term stability of ecosystems exposed to contrasting meteorological events.

Introduction

The global carbon and nutrient cycle in the surface waters of the ocean is strongly driven by marine microbial communities (Falkowski et al., 2008). As microbial communities' function and productivity are directly linked to community diversity and composition (Bell et al., 2005), understanding patterns and processes of community assembly is crucial for the prediction of ecosystem functioning (Nemergut et al., 2013). Microbial community assembly is the outcome of biotic interactions such as competition, predation and mutualism, and abiotic selection by local environmental conditions (Vellend, 2010; Nemergut et al., 2013). In the ocean, there is a general consensus that microbial planktonic communities respond to the physical chemical features of sea water. In temperate and polar regions, these features are strongly associated with the seasonality of the ocean marked by changing temperature regimes (Fuhrman et al., 2015). The dynamics of the ocean may be hard to capture by discrete sampling schemes, and long-term oceanographic time-series studies have proven to be very useful to elucidate links between microbial communities and environmental conditions. Temperature, day length, photosynthetically available radiation, salinity and nutrient concentrations are the main abiotic factors that individually or together strongly impact the seasonal composition of microbial communities (e.g., (Treusch et al., 2009; Eiler et al., 2011; Gilbert et al., 2012; Chow et al., 2013; Cram et al., 2015b; Salter et al., 2015; Parada and Fuhrman, 2017; Auladell et al., 2019; Lambert et al., 2019)). Long term time-series of microbial communities have also shown the importance of biotic forcing (Chow et al., 2014; Ahlgren et al., 2019). Top-down controls, which include predation and viral lysis, and bacteria–bacteria interactions are important factors that shape community assembly. Microbial communities are complex systems of co-occurring species and the use of interaction networks has strongly increased our understanding on the possible connections

between microorganisms within a community (Beman et al., 2011; Steele et al., 2011; Gilbert et al., 2012; Chow et al., 2014; Cram et al., 2015a; Needham et al., 2017).

Time-series studies have demonstrated the strong predictability of microbial community composition season after season, and year after year (Fuhrman et al., 2006). This key feature has been seen repeatedly for bacteria and archaea (Hugoni et al., 2013; Chafee et al., 2018; Galand et al., 2018), but also eukaryotes (Giner et al., 2019), and appears to be maintained under irregular environmental perturbations (Lambert et al., 2019). This strong pattern of re-occurrence has been explained by the invisible hand metaphor, which refers to the cumulative effect of individuals working in their own self-interest that leads to well-regulated community function without any centralized control mechanism (Fuhrman et al., 2015). This long-term pattern has been observed at monthly sampling frequencies and the question remains as to whether such a motif could be seen at higher sampling frequency. Generation times of phytoplankton and marine bacteria can vary a lot, but are estimated to range from a few hours to a few days (Kirchman, 2016). Daily or twice a week sampling would thus better match the biological rhythm of the microbial sea (Fuhrman et al., 2015).

Higher frequency time-series studies have recently emerged and showed the rapid transitions between closely related strains (Needham and Fuhrman, 2016; Ward et al., 2017; Martin-Platero et al., 2018) and recurrent patterns of microdiversity in a coastal ecosystem (Chafee et al., 2018). They have followed the succession of species during blooms over a few months at a daily frequency (Needham and Fuhrman, 2016; Martin-Platero et al., 2018; Needham et al., 2018) or twice a week (Teeling et al., 2012). Only a few have monitored the dynamics of communities over longer time period: one year at a twice a week frequency (Lindh et al., 2015) or 3 years at weekly/twice a week frequency (Ward et al., 2017; Chafee et al., 2018). These studies have focused on prokaryotes and information on the long-term

high frequency dynamics of the 3 domains of life is lacking, and especially for coastal ecosystems.

Temperate coastal ecosystems are impacted by land and particularly in the Mediterranean Sea, where sudden and irregular weather events, such as strong precipitations causing flash flooding, storms triggering sediment resuspension, or wind inducing water column mixing, can have a strong impact (Charles et al., 2005; Thyssen et al., 2014; Tinta et al., 2015). These contrasting weather conditions are predicted to increase with a changing climate (Scoccimarro et al., 2016). The question remains as to whether community successions, and interactions between marine microorganisms, can remain stable under irregular climate events, or if the predicted increases in temperature and strong precipitations could disrupt individual interactions within communities (Berner et al., 2018).

The aim of our study was to investigate the patterns of planktonic picoeukaryote, bacteria and archaea co-occurrences under contrasting environmental conditions. The study was designed to have a sampling frequency that could match both the biological rhythm of marine microbes and the short time scale of extreme events such as flooding and storms. Furthermore, the multiyear sampling was intended to discriminate recurrent microbial community dynamics from stochastic events. We sampled the Banyuls Bay microbial observatory (SOLA), a coastal site of the NW Mediterranean Sea, twice a week during the most productive winter months (January-March) and weekly the rest of the time. Samples in this study included those collected during an “average” year, with physical and chemical parameters close to the long term mean, and two years marked by environmental winter perturbations in terms of seawater temperature and freshwater influx.

Results

Overall community composition, diversity and environmental conditions

A canonical correspondence analysis (CCA) was carried out to compare the composition of communities during the 3 high frequency sampling winter periods for the prokaryote (Fig. 1A) and eukaryote (Fig. 1B). Communities grouped generally by month of sampling but there were some exceptions for both eukaryotes and prokaryotes, in particular samples from December 2016, February 2017 and March 2017 were separated from the others for both domains of life.

In order to precisely identify dissimilarities in community composition, we compared systematically differences between successive samples (i.e. t sample vs t_{+1} sample) for the 3 winter periods (Supplementary Fig. 1). The most important dissimilarities were identified as values above the annual average. They indicate abrupt changes in community composition within a short period of time. Their occurrence was indicated by arrows on top of the environmental conditions (Fig. 1C), and squares around CCA markers (Fig. 1A and B). Seven out of the ten highest dissimilarities in community composition occurred in 2017.

During the winter season, which is the most productive time of the year at the site {Galand, 2015 #2028}, the strong changes in community composition, marked by arrows, corresponded most of the time to changes in salinity, but not always (Fig. 1C). These changes were associated with increased nitrate concentrations and often to higher river discharge (Fig. 1C). This was clearly visible in March 2015 (red arrow), December 2016 (blue arrow), February 2017 (blue arrow) and March 2017 (blue arrow).

The abrupt changes did not, however, impact the annual seasonality of the microbial communities, which was characterized by repeatable temporal patterns in the community composition, as shown by the higher similarity observed between communities sampled one year apart and lower similarity for communities taken 6 months apart for both eukaryotes and prokaryotes (Supplementary Fig. 2).

The Shannon diversity index pattern varied from year to year. Its range of variation was low in 2015, decreased from January to April in 2016, and it was highly variable in 2017 (Supplementary Fig. 3).

Community composition at the class level

Among all the eukaryotic classes found in the dataset, four main classes dominated: *Bacillariophyta*, *Dinophyceae*, *Mamiellophyceae* and *Syndiniales* (Supplementary Fig. 4). Overall, for a given month, the average sequence abundance of these major groups varied from year to year (Fig. 2). *Bacillariophyta*, which showed relatively low levels of average sequence abundance throughout the sampling period, were more abundant in February and March 2017. *Bacillariophyta* were almost absent in March 2016. Average abundance of *Dinophyceae* remained relatively stable during the three years of sampling, with higher levels in January and February 2017. *Mamiellophyceae* had more variable patterns of abundance. In 2015, they were more abundant in January and February, in 2016 they were more abundant in March, and in 2017 in January. *Mamiellophyceae* were mainly composed of the genera *Bathycoccus* and *Micromonas*. These two picoeukaryotes had different dynamics characterized by a *Micromonas* bloom in early winter followed by *Bathycoccus* (ASV5 vs ASV 4, Supplementary Fig. 5). *Syndiniales* abundance did not vary much in 2015, unlike in 2016 and 2017 when they were more abundant in March, and January/March respectively.

For prokaryotes, abundance of the main classes also varied from year to year and especially in 2017 (Fig. 2). For *Alphaproteobacteria* decreases in abundance were seen in February and March 2017. *Cyanobacteria* average abundances were relatively low and stable during the three years of sampling, except for an increase in March 2017. Average abundance for *Flavobacteria* in 2015 and 2016 showed an increase in March for both years.

Flavobacteria, in contrast, had a higher than average relative abundance in February 2017. Finally, *Gammaproteobacteria* had similar levels of abundance between years from January to March, except for February 2017 when they were less abundant (Fig. 2).

Co-occurrence networks

The co-occurrences of ASVs was investigated for each high frequency sampling winter seasons (January, February and March) by network analysis based on the Maximal Information Coefficient (MIC). MIC identifies correlations between variables and is best adapted to the non-linear temporal nature of the data (Reshef et al., 2011). The networks, based on significant MIC values ($p>0.05$) with a false discovery rate (FDR) of 5%, show that there were clear differences in the topology between years (Fig. 3). The 2015 network was narrower, more clustered and more centralized than the 2016 and 2017 networks (Supplementary Table 3).

The 2015 network was composed of 2 main modules, with a modularity of 12.4 and 5.7, respectively, as well as 4 smaller modules (modularity<1) (Supplementary Table 4). The ASVs that were more abundant in January and February grouped in one module (Fig. 3A). In January, the hub ASVs defined as the nodes with highest degree, belonged first to *Euryarchaeota* Marine Group II (Archaea), and then a number of Eukaryotes including *Syndiniales*, diatoms (*Chaetoceros brevis*), a flagellate (*Florenciella parvula*) and *Micromonas* (Mamiellophyceae) (Supplementary Table 5, Fig 3A). The hub ASVs of February belonged to *Acidimicrobiales* (OM1 clade), *Gammaproteobacteria* clades ZD0405 and SAR86, and diatoms (*Chaetoceros curvisetus*). The second main module was composed of ASVs abundant in March and included SAR11 surface 1 clade (*Alphaproteobacteria*), *Flavobacteriales, Rhodobacteraceae* and *Syndiniales* (Eukaryota) as hubs. The 2015 network

did not show any discernible pattern with respect to temperature or salinity, but the highest values were associated with the January ASVs (Fig. 3B, 3C).

The 2016 network consisted of 3 modules with a modularity of 14.5, 6 and 3, respectively and followed a seasonal pattern, but with a distinct March module (Fig. 3A, Supplementary Table 4). In January, the hub ASVs belonged to the cyanobacteria *Prochlorococcus, Acidimicrobiales* OM1 clade, *Deltaproteobacteria* SAR324 clade, the SAR11 surface 2 clade (*Alphaproteobacteria*) and to the dinoflagelate *Gymnodiniales*. In the February group, the hubs were diatoms from the *Florenciellales* and Raphid-pennate families, *Flavobacteriales* of the NS9 marine group and Syndiniales. The second module contained ASVs that were more abundant in March. The hub ASVs were members of the *Flavobacteriaceae*, MAST 6 (Stramenopiles), and Syndiniales (Supplementary Table 5). *Micromonas* (*Mamiellophyceae*) was connected with both modules (Fig. 3). The 2016 network was separated into a low temperature (11-12°C) and a high temperature (13-14°C) module (Fig. 3B), and the ASVs were mainly related to samples with higher salinity (38) (Fig. 3C).

The 2017 network formed 8 low modularity modules (modularity between 4.4 and 0.5) (Fig. 3, Supplementary Table 4). A seasonal pattern within the ASVs was not as clear as in 2015 and 2016. In January, abundant hub ASVs belonged to *Micromonas* (*Mamiellophyceae*), *Thaumarchaeota* Marine group I (Archaea) and the flagellate algae *Pelagomonas* (Supplementary Table 5). The ASVs abundant in February were separated in 2 groups. On the top of the network (Fig. 3A), diatoms (*Skeletonema*) were abundant, and the hubs belonged to *Flavobacteriales* and, among Eukaryotes, *Lauderia* diatoms and the phagotrophic flagellate *Ebria* (Cercozoa). In the second part of the network containing ASVs abundant in February, a Syndiniales was abundant. The ASVs that were abundant in March were in the middle of the network and the hubs were identified as *Synechococcus*

cyanobacteria, *Flavobacteriaceae* and the flagellate *Chrysochromulinaceae*. The 2017 network showed a central module with higher temperature (13°C), surrounded by lower temperature modules (12°C) (Fig 3B). It was composed of modules of ASVs found under average salinity of 37, and one module of low salinity ASVs (35) (Fig. 3C).

ASV co-occurrences

In the networks, a total of 42 ASVs were common to the three high frequency winter samplings (Supplementary Fig. 6). In order to assess if the first neighbor nodes of the 42 common ASVs changed from year to year, we represented the positive co-occurrences in radar plots (Fig. 4). The radius of the spider net corresponds to the MIC score between the central ASV and its first neighbors.

Noteworthy, all of the 42 ASVs changed neighbors between years. The number of first neighbors also changed from year to year (Fig. 4, Supplementary Table 6). Overall, the total number of first neighbors decreases from 2015 to 2017 (542, 389 and 263 in 2015, 2016 and 2017 respectively). Half of the ASV (21) had a larger number of first neighbors in 2015 compared to the other years. A total of 16 ASVs had more first neighbors in 2016 and only 2 had more neighbors in 2017. Three ASVs had years with similar number of neighbors (Fig. 4). The total number of neighbors per year varied greatly between ASVs. The highest values were 51 for ASV38 (*Alphaproteobacteria*) and the lowest 6 for ASV10 (*Flavobacteria*) (Fig. 4, Supplementary Table 6).

Among the common ASVs, 23 were earlier identified as rhythmic over 7 years (Lambert et al., 2019) (marked by a black frame, Fig. 4). They also had first neighbors that varied in number and identity between years (Fig. 4). Finally, bacterial ASVs were mostly

associated with bacteria (59% of the first neighbors) while eukaryotic ASVs were mostly associated with eukaryotes (67% of the first neighbors). However, the affiliation of the first neighbor to a given domain of life also changed from year to year. For a given ASV, some years showed more eukaryotic first neighbors while other displayed more prokaryotic neighbors.

Discussion

Our high frequency sampling study, focusing on the productive winter months, showed that the patterns of the microbial networks linking members of the 3 domains of life changed from year to year. To the best of our knowledge, inter-annual variations of network topology have not been shown earlier. On the contrary, a recent high frequency sampling study from the North Sea reported that network topologies were similar for co-varying microbes between two different years for a same season (Chafee et al., 2018). Networks have, however, been shown to change between seasons in both freshwater (Kara et al., 2013; Hu et al., 2017) and marine environments (Chafee et al., 2018; Cui et al., 2019). Different temporal patterns in network topology have also been observed along shorter time series (Martin-Platero et al., 2018). These temporal changes reflect variations in community composition with changing environmental conditions along a year (Fuhrman et al., 2015). Nevertheless, these earlier studies did not test the year to year stability of the networks. Many correlation-based association networks have focused only on the overall trend of microbial interconnectivity without distinguishing seasons and years, the goal being to identify time-dependent associations among ecologically important taxa (Steele et al., 2011; Chow et al., 2013; Needham et al., 2013; Chow et al., 2014; Cram et al., 2015a; Milici et al., 2016; Needham et

al., 2017; Parada and Fuhrman, 2017). The fact that network topologies can change from year to year should be considered in future temporal studies.

The long-term stability of co-occurrences has not been tested earlier. Co-occurrences could have been considered to be robust and maintained over time since similar microbial communities have been shown to reoccur, at a same site, year after year (Fuhrman et al., 2006; Gilbert et al., 2012; Lambert et al., 2019). We also observed annual patterns of reoccurrence, but our data revealed that despite these reproducible patterns, the microbial networks are not necessarily robust as their topology can be broken when climatic conditions changes.

Interestingly, the abrupt or gradual changes (salinity and temperature) that we observed did not impact the overall rhythmicity of the microbial sea over the long term (Lambert et al., 2019) nor in this study. Regardless of the environmental perturbations, some ASVs reoccur every year. However, here we observed that these reoccurring ASVs rarely had the same first neighbors, which indicate very strong changes of co-occurrence patterns from year to year. The changing patterns probably correspond to the changing environmental conditions that included higher sea water temperature in 2015-2016 and numerous salinity drops in 2016-2017. Strong changes were also seen in the overall number of first neighbors within a network, which was halved from 2015 to 2017. Nodes with fewer neighbors may be an indication of a less robust network (Röttjers and Faust, 2018) and may thus illustrate a possible weakening of the network of co-occurrence by environmental perturbations.

The observed changes in co-occurrence patterns may have different explanations. First, if we hypothesize that co-occurrences represent interactions between microorganisms, such as cross feeding, predation or parasitism (Fuhrman et al., 2015), it could mean that some species might be replaced by others having a similar function. It could be the case for *Micromonas* (ASV5) that co-occurred with different potential ciliate predators between 2015

and 2017. The possibility for a partial functional redundancy at the individual level has been described earlier (Galand et al., 2018). Although there may not be functional redundancy at the community level (Galand et al., 2018), at the individual level, a switch between different organisms that have a same specific function is possible. In our study, a gene level functional redundancy may exist for the *Rhodobacterales* and the *Oceanospirillales*, or the *Thaumarchaeota*, which all could produce B12 (Doxey et al., 2015; Gómez-Consarnau et al., 2018), and that change co-occurrences with the *Mamiellophyceae* that are B12 auxotrophs (Bathycoccus ASV_euk4, Micromonas ASV_euk22). Our study is, however, focused on the small size fraction of the microbial communities and thus misses larger planktonic organisms. Phytoplankton is known to interact with prokaryotes, but these interactions, and their possible stability over time, cannot be accounted for in our analysis.

The other hypothesis for the change of neighbors is that there are only limited interactions between species, and that the co-occurrence patterns only represent species having preferences for similar environmental conditions, i.e they share similar niches. This would imply that the strong seasonal patterns, such as the ones observed for dominant ASVs like *Mamiellophyceae* or SAR11, would be driven by structuring environmental parameters like temperature and day length (Gilbert et al., 2012; Lambert et al., 2019). The reality probably reflects a mix of both hypotheses with the presence of microorganisms that are unfaithful in their interactions, and cohorts that respond to similar environmental conditions.

The abrupt perturbations that we observed at the Banyuls microbial observatory (SOLA) were characterized by lower sea water salinity. These drops corresponded to episodes of heavy rain leading to higher water level in the local river. Large rivers further up the coast have also been shown to impact the study site (Laghdass et al., 2010). Episodes of heavy rain are often concomitant with storms in the North Eastern Mediterranean (Charles et al., 2005; Guizien et al., 2007). Storms mix the sea floor sediments through the water column,

347 which increases nutrient concentrations. Nutrients are also brought from land by the river and
348 can induce blooms measured as peak of chlorophyll, as seen earlier along the coast of the
349 eastern Mediterranean (Charles et al., 2005; Nunes et al., 2018).
350 At the Banyuls site, the strongest low salinity events were observed during winter 2016-2017.
351 The perturbations resulted in lower relative abundance of the predominant marine bacteria
352 SAR11 (*Alphaproteobacteria*) and an increase of *Flavobacteria*. Among picoeukaryotes, the
353 parasitic *Syndiniales* increased in relative abundance. The corresponding microbial network
354 was characterized by a low salinity module that was composed of diatoms of the genus
355 *Skeletonema* and *Lauderia*, and highly connected bacteria of the family *Flavobacteriaceae*
356 and *Rhodobacteracea*. Our results suggest that the freshwater input, and the associated
357 nutrients, favored the bloom of specific diatoms species that were co-occurring with bacteria
358 that are usually not abundant in the Bay of Banyuls at that time of the year. These bacteria
359 have been seen associated with diatom blooms earlier (Teeling et al., 2016), and diatoms
360 have been shown to bloom following episodic fertilization events associated with freshwater
361 runoff (Tinta et al., 2015; Nunes et al., 2018). *Skeletonema* in particular was observed to
362 bloom following heavy rains along the Catalan coast (Estrada, 1979). It should, however, be
363 noted that microorganisms like diatoms are not expected to pass through our 3 µm filters. The
364 fact that we detected sequences from larger cells suggests that DNA from damaged or lysed
365 organisms passed through the pre-filter. The interpretation of the co-occurrence patterns is
366 thus done within the frame of this technical limitation.
367 Winter 2015-2016 was characterized by higher sea water temperatures in January and
368 February compared to average. These higher temperatures may have impacted the bloom of
369 *Micromonas* that took place later that year compared to average (February instead of
370 January). They may have been replaced by Cyanobacteria (*Prochlorococcus*) that increased
371 in sequence abundance and became hub species in the network in January. *Prochlorococcus*

372 are overall less abundant than *Synechococcus* in the NW Mediterranean Sea (Schauer et al.,
373 2003), but appear to bloom in autumn when solar radiations are weaker (Sommaruga et al.,
374 2005). Our results suggest that when sea water temperature remains relatively high in early
375 winter, the bloom of *Prochlorococcus* can persist at the expense of *Micromonas*
376 development. Such a switch could have an impact on the functioning of the coastal NW
377 Mediterranean. It has, for example, been shown that after a mild winter in the Baltic Sea the
378 spring bloom was reduced, thus impacting the carbon cycle (Legrand et al., 2015). Such a
379 scenario could lead to lower carbon export to the marine food web (Berner et al., 2018).
380 Winter 2014-2015 had environmental conditions that were the most similar to an
381 average year. The corresponding microbial network was marked by a clear separation
382 between seasonal modules. It corresponded to the temporal succession of species in the
383 coastal NW Mediterranean, which is marked by a strong seasonality (Hugoni et al., 2013;
384 Galand et al., 2018; Lambert et al., 2019). In January, the hub species were picoeukaryotes
385 identified as *Micromonas* (class *Mamiellophyceae*), *Euryarchaeota* Marine Group II
386 (*Archaea*), and diatoms (*Chaetoceros brevis*). A *Micromonas* bloom at the beginning of the
387 year has been seen earlier at the Banyuls site (Lambert et al., 2019), but its co-occurrence
388 with *Euryarchaeota* has not been reported. In February, the communities were characterized
389 by diatoms of the genus *Chaetoceros* and bacteria belonging to the ZD0405 and SAR86
390 clades of *Gammaproteobacteria*. These bacteria have been reported as associated with
391 diatom blooms earlier (Lucas et al., 2015; Teeling et al., 2016). In March, the hub species
392 corresponded to classical pelagic microbial communities composed of the SAR11 surface 1
393 clade (*Alphaproteobacteria*) and *Bathycoccus* for the pico-eukaryotes, which is known to
394 bloom in late winter at the site (Lambert et al., 2019). As *Bathycoccus* and SAR11 are both
395 auxotroph to vitamin B1 precursors, their co-occurrence may reflect shared ecological niches

rather than interaction as proposed for co-occurring *Micromonas* and SAR11 (Lambert et al., 2019).

Conclusions

Our high frequency sampling of NW Mediterranean microbial communities revealed that co-occurrence networks of picoeukaryote, bacteria and archaea changed from year to year. Weather perturbations in temperature or salinity seem to alter the topology of the microbial networks. In addition, individual taxa changed neighbor from year to year suggesting an unfaithful relationship between marine microorganisms. However, the global seasonal patterns of rhythmic ASVs were maintained, which indicates that the communities recover from these perturbations. It implies a strong environmental control, but it also suggests that changing co-occurrences between marine microorganisms may allow the long-term stability of the ecosystem. The resilience of seasonal microbial ecosystems remains, however, to be assessed under the more extreme climatic events predicted for the future. Well-established time series are essential for the monitoring of anthropological impacts on the sea and to get a good understanding of the functioning of the microbial ocean.

Experimental Procedures

Sampling

Surface water (3m) was collected with Niskin bottles from January 2015 to March 2017 at the Banyuls Bay microbial observatory (SOLA) (42°31′N, 03°11′E) in the Bay of Banyuls-sur-Mer, North Western Mediterranean Sea, France. A total of 5 L of seawater was prefiltered through 3 µm pore-size polycarbonate filters (Merck-Millipore, Darmstadt, Germany), and the microbial biomass was collected on 0.22-µm pore-size GV Sterivex

cartridges (Merck-Millipore) and stored at -80 °C until nucleic acid extraction. Samples were collected twice a week during winters: January to March 2015, January to April 2016 and December 2016 to March 2017, and once a week otherwise (spring, summer and autumn). The physicochemical (temperature, salinity, day length, nitrate, nitrite, silicate and phosphate concentrations) and biological (chlorophyll a) were provided by the Service d'Observation en Milieu Littoral (SOMLIT). The levels of the river discharging in the bay of Banyuls, the Baillaury, were obtained from the "Service Central d'Hydrométéorologie et d'Appui à la Prévision des Inondations" (http://www.hydro.eaufrance.fr/).

DNA extraction, amplification and sequencing

The nucleic acid extraction followed protocols published earlier (Lambert et al., 2019). To summarize, the Sterivex filters were thawed on ice, followed by addition of lysis buffer (40nM EDTA, 50nM Tris, 0.75M sucrose) and 25 µL of lysozyme (20 mg mL^{-1}). The filters were then incubated for 45 minutes at 37°C on a rotary mixer. Subsequently, 8µL of Proteinase K (20mg mL^{-1}) and 26µL of sodium dodecyl sulfate (20% v/v) were added before incubating for 1 hour at 55°C. Total DNA was then extracted and purified with the Qiagen AllPrep kit (Qiagen, Hilden, Germany) following the kit's protocol.

Specific primers were used to target the eukaryotic V4 region (TAReuk_F1 [5'-CCAGCASCYGCGGTAATTCC] and TAReuk_R [5'-ACTTTCGTTCTTGATYRATGA], (Stoeck et al., 2010) and the prokaryotic V4-V5 region (515F-Y [5'-GTGYCAGCMGCCGCGGTAA] and 926R [5'-CCGYCAATTYMTTTRAGTTT] (Parada et al., 2016). Library preparation and sequencing were carried out by the Genotoul platform (Toulouse, France), with the Illumina Miseq 2x250 bp kits. All sequences were deposited in NCBI under accession number PRJNA579489.

Sequence analysis and preprocessing

The standard pipeline of the DADA2 package (v1.6) (Callahan et al., 2016) in "R" was used to do the analysis of the raw sequences. The parameters used for the eukaryote dataset were: trimLeft=c(20, 21) ,truncLen=c(250,250), maxN=0, maxEE=c(2,2), truncQ=2; and for the prokaryote dataset: trimLeft=c(19, 20), truncLen=c(240,200), maxN=0, maxEE=c(2,5), truncQ=2. We analyzed 141 and 142 samples for the eukaryote and prokaryote datasets respectively, and obtained a total of 3.8 and 3.4 million reads respectively after DADA2 data processing (Supplementary Table 1). The taxonomy assignment was done with the The Protist Ribosomal Reference database (PR^2)v.4.10.0 (Guillou et al., 2012) database for the eukaryotes and with SILVA v.128 database (Quast et al., 2013) for the prokaryote. The "assignTaxonomy" function in DADA2 implements the RDP naive Bayesian classifier method (Wang et al., 2007).

Taxa belonging to the supergroup "Opisthokonta" were removed from the eukaryote dataset and taxa belonging to eukaryotes were removed from the prokaryote dataset. Samples containing less than 5000 reads and 9000 reads were removed from the eukaryote and prokaryote dataset respectively. A total of 139 and 137 samples remained for the eukaryotes and the prokaryotes respectively. These preprocessing steps were done with the "R" package "Phyloseq" (McMurdie and Holmes, 2013).

Microbial communities in this study and in our previous study (Lambert et al., 2019) were not amplified with the same primer set. Here we chose to use universal primers shown to have a good coverage of both Bacteria and Archaea (Parada et al., 2016) instead of the two sets of separate primers used earlier (Lambert et al., 2019). In order to identify in this study the ASVs that were detected as rhythmic in our previous study, we compared both datasets by BLAST (Altschul et al., 1997) (blastn, >99% identity). For the eukaryotes, reads from both studies overlapped (~230 bp), and we could thus do a direct identification

(Supplementary Table 2). For the prokaryotes, however, the reads did not have an overlapping region. We therefore did a first BLAST of the rhythmic prokaryotic ASVs (Lambert et al., 2019) against the SILVA v.128 database. The matching sequences were then extracted from SILVA to create a novel custom database. Finally, we did a BLAST of the prokaryotic ASVs from this study against the custom database (Supplementary Table 2). We could then identify the ASVs from Lambert et al 2019 and the ASVs from this study that exactly matched the same SILVA reference sequence.

Statistics

Sequence counts for both datasets were normalized with the median-ratio method implemented in the "DESeq2" package (Love et al., 2014), which is mathematically equivalent to the compositional log-ratio (clr) transformation that accounts for the compositional nature of the data (Quinn et al., 2018).

The Bray-Curtis dissimilarity index was calculated with the "vegdist" function of the "Vegan" package (Oksanen et al., 2019) in "R". Distances between samples were calculated based on community composition with a canonical correspondence analyses (CCA) with the "Vegan" package in "R". Contribution of environmental factors were added as arrows.

Abrupt changes in community composition between two samples were identified as Bray-Curtis dissimilarity values peaking above average. For that purpose, the Bray-Curtis dissimilarity index was calculated between two successive samples (t vs t_{+1}), within each dataset, to identify variations of community composition with time.

Networks were based on the Maximal Information Coefficient (MIC), a measure that effectively identifies relationships between variables and that is best adapted to the non-linear temporal nature of the data, and behave well with small datasets (Reshef et al., 2011). The MIC was computed for each year based on ASV tables containing the most abundant ASVs.

They were selected as the 20 most abundant ASVs per sample, in each dataset, over each winter period (January, February, March), and represented over all a total of 153 ASVs in 2015, 182 in 2016 and 187 in 2017. The MIC was then used to build a network that was visualized in Cytoscape (Shannon et al., 2003). The full network was pruned to visualize ASV interactions that had a Pearson linear regression > 0 (positive interactions) and a MIC > 0.75. These MIC values corresponded to significant interactions ($p<0.05$) when accepting a false discovery rate (FDR) of 5% at most as computed with MICtools (Albanese et al., 2018). The layout chosen for the network was edge-weighted spring embedded, using the MIC parameter. Module analyses were done with the CytoCluster app (Li et al., 2017) for Cytoscape, using the HC-PIN clustering algorithm with the default parameters (Weak, Threshold: 2.0 and ComplexSize Threshold: 3). Network analysis was done using the NetworkAnalyzer tool included in Cytoscape. Hub ASVs, which are the ones associated with a high number of other ASVs, were defined for each network as the nodes with highest degree (Röttjers and Faust, 2018). The networks were treated as undirected.

Radar plots were made with the "fmsb" package (https://cran.r-project.org/web/packages/fmsb) in "R". The heatmap was made with the "Phyloseq" package. For this figure, the eukaryotic and prokaryotic datasets were merged. Only ASVs with more than 10 reads were represented.

Acknowledgments

We are grateful to the captain and the crew of the RV 'Nereis II' for their help in acquiring the samples. We thank the "Service d'Observation", particularly Eric Maria and Paul Labatut, for their help in obtaining and processing of the samples. SL was supported by a PhD fellowship from the doctoral school ED129. This work was supported by the French Agence

Nationale de la Recherche through the projects Photo-Phyto (ANR-14-CE02-0018) to FYB, and EUREKA (ANR-14-CE02-0004-01) to PEG.

References:

Ahlgren, N.A., Perelman, J.N., Yeh, Y.C., and Fuhrman, J.A. (2019) Multi-year dynamics of fine-scale marine cyanobacterial populations are more strongly explained by phage interactions than abiotic, bottom-up factors. Environ Microbiol 21: 2948-2963.

Albanese, D., Riccadonna, S., Donati, C., and Franceschi, P. (2018) A practical tool for maximal information coefficient analysis. GigaScience 7: 1-8.

Altschul, S.F., Madden, T.L., Schaffer, A.A., Zhang, J., Zhang, Z., and Miller, W. (1997) Gapped BLAST and PSI-BLAST: a new generation of protein database search programs. Nucleic Acids Res 25: 3389-3402.

Auladell, A., Sánchez, P., Sánchez, O., Gasol, J.M., and Ferrera, I. (2019) Long-term seasonal and interannual variability of marine aerobic anoxygenic photoheterotrophic bacteria. ISME J: 1.

Bell, T., Newman, J.A., Silverman, B.W., Turner, S.L., and Lilley, A.K. (2005) The contribution of species richness and composition to bacterial services. Nature 436: 1157-1160.

Beman, J.M., Steele, J.A., and Fuhrman, J.A. (2011) Co-occurrence patterns for abundant marine archaeal and bacterial lineages in the deep chlorophyll maximum of coastal California. ISME J 5: 1077.

Berner, C., Bertos-Fortis, M., Pinhassi, J., and Legrand, C. (2018) Response of Microbial Communities to Changing Climate Conditions During Summer Cyanobacterial Blooms in the Baltic Sea. Front Microbiol 9: 1562.

Callahan, B.J., McMurdie, P.J., Rosen, M.J., Han, A.W., Johnson, A.J.A., and Holmes, S.P. (2016) DADA2: high-resolution sample inference from Illumina amplicon data. Nat Methods 13: 581.

Chafee, M., Fernàndez-Guerra, A., Buttigieg, P.L., Gerdts, G., Eren, A.M., Teeling, H., and Amann, R.I. (2018) Recurrent patterns of microdiversity in a temperate coastal marine environment. ISME J 12: 237.

Charles, F., Lantoine, F., Brugel, S., Chrétiennot-Dinet, M.-J., Quiroga, I., and Rivière, B. (2005) Seasonal survey of the phytoplankton biomass, composition and production in a littoral NW Mediterranean site, with special emphasis on the picoplanktonic contribution. Estuar Coast Shelf Sci 65: 199-212.

Chow, C.-E.T., Kim, D.Y., Sachdeva, R., Caron, D.A., and Fuhrman, J.A. (2014) Top-down controls on bacterial community structure: microbial network analysis of bacteria, T4-like viruses and protists. ISME J 8: 816.

Chow, C.-E.T., Sachdeva, R., Cram, J.A., Steele, J.A., Needham, D.M., Patel, A. et al. (2013) Temporal variability and coherence of euphotic zone bacterial communities over a decade in the Southern California Bight. ISME J 7: 2259-2273.

Cram, J.A., Xia, L.C., Needham, D.M., Sachdeva, R., Sun, F., and Fuhrman, J.A. (2015a) Cross-depth analysis of marine bacterial networks suggests downward propagation of temporal changes. ISME J 9: 2573.

564 Cram, J.A., Chow, C.-E.T., Sachdeva, R., Needham, D.M., Parada, A.E., Steele, J.A., and
565 Fuhrman, J.A. (2015b) Seasonal and interannual variability of the marine bacterioplankton
566 community throughout the water column over ten years. ISME J 9: 563.
567 Cui, Y., Chun, S.-J., Baek, S.H., Lee, M., Kim, Y., Lee, H.-G. et al. (2019) The water depth-
568 dependent co-occurrence patterns of marine bacteria in shallow and dynamic Southern Coast,
569 Korea. Sci Rep 9: 1-13.
570 Doxey, A.C., Kurtz, D.A., Lynch, M.D.J., Sauder, L.A., and Neufeld, J.D. (2015) Aquatic
571 metagenomes implicate Thaumarchaeota in global cobalamin production. ISME J 9: 461-471.
572 Eiler, A., Hayakawa, D.H., and Rappé, M.S. (2011) Non-random assembly of
573 bacterioplankton communities in the subtropical North Pacific Ocean. Front Microbiol 2:
574 140.
575 Estrada, M. (1979) Observaciones sobre la heterogeneidad del fitoplancton en una zona
576 costera del mar Catalán. Inv Pesq 43: 637-666.
577 Falkowski, P.G., Fenchel, T., and Delong, E.F. (2008) The microbial engines that drive
578 Earth's biogeochemical cycles. Science 320: 1034-1039.
579 Fuhrman, J.A., Cram, J.A., and Needham, D.M. (2015) Marine microbial community
580 dynamics and their ecological interpretation. Nat Rev Micro 13: 133-146.
581 Fuhrman, J.A., Hewson, I., Schwalbach, M.S., Steele, J.A., Brown, M.V., and Naeem, S.
582 (2006) Annually reoccurring bacterial communities are predictable from ocean conditions.
583 Proc Natl Acad Sci USA 103: 13104-13109.
584 Galand, P.E., Pereira, O., Hochart, C., Auguet, J.C., and Debroas, D. (2018) A strong link
585 between marine microbial community composition and function challenges the idea of
586 functional redundancy. ISME J 12: 2470.
587 Gilbert, J.A., Steele, J.A., Caporaso, J.G., Steinbrück, L., Reeder, J., Temperton, B. et al.
588 (2012) Defining seasonal marine microbial community dynamics. ISME J 6: 298-308.
589 Giner, C.R., Balagué, V., Krabberød, A.K., Ferrera, I., Reñé, A., Garcés, E. et al. (2019)
590 Quantifying long-term recurrence in planktonic microbial eukaryotes. Mol Ecol 28: 923-935.
591 Gómez-Consarnau, L., Sachdeva, R., Gifford, S.M., Cutter, L.S., Fuhrman, J.A.,
592 Sañudo-Wilhelmy, S.A., and Moran, M.A. (2018) Mosaic patterns of B-vitamin synthesis
593 and utilization in a natural marine microbial community. Environ Microbiol 20: 2809-2823.
594 Guillou, L., Bachar, D., Audic, S., Bass, D., Berney, C., Bittner, L. et al. (2012) The Protist
595 Ribosomal Reference database (PR2): a catalog of unicellular eukaryote Small Sub-Unit
596 rRNA sequences with curated taxonomy. Nucleic Acids Res 41: D597-D604.
597 Guizien, K., Charles, F., Lantoine, F., and Naudin, J.-J. (2007) Nearshore dynamics of
598 nutrients and chlorophyll during Mediterranean-type flash-floods. Aquat Living Resour 20:
599 3-14.
600 Hu, A., Ju, F., Hou, L., Li, J., Yang, X., Wang, H. et al. (2017) Strong impact of
601 anthropogenic contamination on the co-occurrence patterns of a riverine microbial
602 community. Environ Microbiol 19: 4993-5009.
603 Hugoni, M., Taib, N., Debroas, D., Domaizon, I., Jouan Dufournel, I., Bronner, G. et al.
604 (2013) Structure of the rare archaeal biosphere and seasonal dynamics of active ecotypes in
605 surface coastal waters. Proc Natl Acad Sci USA 110: 6004-6009.
606 Kara, E.L., Hanson, P.C., Hu, Y.H., Winslow, L., and McMahon, K.D. (2013) A decade of
607 seasonal dynamics and co-occurrences within freshwater bacterioplankton communities from
608 eutrophic Lake Mendota, WI, USA. ISME J 7: 680-684.
609 Kirchman, D.L. (2016) Growth rates of microbes in the oceans. Annu Rev Mar Sci 8: 285-
610 309.
611 Laghdass, M., West, N.J., Batailler, N., Caparros, J., Catala, P., Lantoine, F. et al. (2010)
612 Impact of lower salinity waters on bacterial heterotrophic production and community
613 structure in the offshore NW Mediterranean Sea. Environ Microbiol Rep 2: 761-769.

Lambert, S., Tragin, M., Lozano, J.-C., Ghiglione, J.-F., Vaulot, D., Bouget, F.-Y., and Galand, P.E. (2019) Rhythmicity of coastal marine picoeukaryotes, bacteria and archaea despite irregular environmental perturbations. ISME J 13: 388-401.
Legrand, C., Fridolfsson, E., Bertos-Fortis, M., Lindehoff, E., Larsson, P., Pinhassi, J., and Andersson, A. (2015) Interannual variability of phyto-bacterioplankton biomass and production in coastal and offshore waters of the Baltic Sea. AMBIO 44: 427-438.
Li, M., Li, D., Tang, Y., Wu, F., and Wang, J. (2017) CytoCluster: A cytoscape plugin for cluster analysis and visualization of biological networks. Int J Mol Sci 18: 1880.
Lindh, M.V., Sjöstedt, J., Andersson, A.F., Baltar, F., Hugerth, L.W., Lundin, D. et al. (2015) Disentangling seasonal bacterioplankton population dynamics by high-frequency sampling. Environ Microbiol 17: 2459-2476.
Love, M.I., Huber, W., and Anders, S. (2014) Moderated estimation of fold change and dispersion for RNA-seq data with DESeq2. Genome Biol 15: 550.
Lucas, J., Wichels, A., Teeling, H., Chafee, M., Scharfe, M., and Gerdts, G. (2015) Annual dynamics of North Sea bacterioplankton: seasonal variability superimposes short-term variation. FEMS Microbiol Ecol 91: fiv099.
Martin-Platero, A.M., Cleary, B., Kauffman, K., Preheim, S.P., McGillicuddy, D.J., Alm, E.J., and Polz, M.F. (2018) High resolution time series reveals cohesive but short-lived communities in coastal plankton. Nat Commun 9: 266.
McMurdie, P.J., and Holmes, S. (2013) phyloseq: an R package for reproducible interactive analysis and graphics of microbiome census data. PloS one 8: e61217.
Milici, M., Deng, Z.-L., Tomasch, J., Decelle, J., Wos-Oxley, M.L., Wang, H. et al. (2016) Co-occurrence analysis of microbial taxa in the Atlantic Ocean reveals high connectivity in the free-living bacterioplankton. Front Microbiol 7: 649.
Needham, D.M., and Fuhrman, J.A. (2016) Pronounced daily succession of phytoplankton, archaea and bacteria following a spring bloom. Nat Microbiol 1: 16005.
Needham, D.M., Sachdeva, R., and Fuhrman, J.A. (2017) Ecological dynamics and co-occurrence among marine phytoplankton, bacteria and myoviruses shows microdiversity matters. ISME J 11: 1614.
Needham, D.M., Chow, C.-E.T., Cram, J.A., Sachdeva, R., Parada, A., and Fuhrman, J.A. (2013) Short-term observations of marine bacterial and viral communities: patterns, connections and resilience. ISME J 7: 1274-1285.
Needham, D.M., Fichot, E.B., Wang, E., Berdjeb, L., Cram, J.A., Fichot, C.G., and Fuhrman, J.A. (2018) Dynamics and interactions of highly resolved marine plankton via automated high-frequency sampling. ISME J 12: 2417.
Nemergut, D.R., Schmidt, S.K., Fukami, T., O'Neill, S.P., Bilinski, T.M., Stanish, L.F. et al. (2013) Patterns and processes of microbial community assembly. Microbiol Mol Biol Rev 77: 342-356.
Nunes, S., Latasa, M., Gasol, J.M., and Estrada, M. (2018) Seasonal and interannual variability of phytoplankton community structure in a Mediterranean coastal site. Mar Ecol Prog Ser 592: 57-75.
Oksanen, J., Blanchet, F.G., Kindt, R., Legendre, P., Minchin, P.R., O'hara, R. et al. (2019) Package 'vegan'. Community ecology package, version 2.5-6.
Parada, A.E., and Fuhrman, J.A. (2017) Marine archaeal dynamics and interactions with the microbial community over 5 years from surface to seafloor. ISME J 11: 2510-2525.
Parada, A.E., Needham, D.M., and Fuhrman, J.A. (2016) Every base matters: assessing small subunit rRNA primers for marine microbiomes with mock communities, time series and global field samples. Environ Microbiol 18: 1403-1414.

662 Quast, C., Pruesse, E., Yilmaz, P., Gerken, J., Schweer, T., Yarza, P. et al. (2013) The
663 SILVA ribosomal RNA gene database project: improved data processing and web-based
664 tools. Nucleic Acids Res 41: D590-D596.
665 Quinn, T.P., Erb, I., Richardson, M.F., and Crowley, T.M. (2018) Understanding sequencing
666 data as compositions: an outlook and review. Bioinformatics (Oxford, England) 34: 2870-
667 2878.
668 Reshef, D.N., Reshef, Y.A., Finucane, H.K., Grossman, S.R., McVean, G., Turnbaugh, P.J. et
669 al. (2011) Detecting Novel Associations in Large Data Sets. Science 334: 1518-1524.
670 Röttjers, L., and Faust, K. (2018) From hairballs to hypotheses–biological insights from
671 microbial networks. FEMS Microbiol Rev 42: 761-780.
672 Salter, I., Galand, P.E., Fagervold, S.K., Lebaron, P., Obernosterer, I., Oliver, M.J. et al.
673 (2015) Seasonal dynamics of active SAR11 ecotypes in the oligotrophic Northwest
674 Mediterranean Sea. ISME J 9: 347-360.
675 Schauer, M., Balagué, V., Pedrós-Alió, C., and Massana, R. (2003) Seasonal changes in the
676 taxonomic composition of bacterioplankton in a coastal oligotrophic system. Aquat Microb
677 Ecol 31: 163-174.
678 Scoccimarro, E., Gualdi, S., Bellucci, A., Zampieri, M., and Navarra, A. (2016) Heavy
679 precipitation events over the Euro-Mediterranean region in a warmer climate: results from
680 CMIP5 models. Reg Environ Change 16: 595-602.
681 Shannon, P., Markiel, A., Ozier, O., Baliga, N.S., Wang, J.T., Ramage, D. et al. (2003)
682 Cytoscape: a software environment for integrated models of biomolecular interaction
683 networks. Genome research 13: 2498-2504.
684 Sommaruga, R., Hofer, J.S., Alonso-Sáez, L., and Gasol, J.M. (2005) Differential sunlight
685 sensitivity of picophytoplankton from surface Mediterranean coastal waters. Appl Environ
686 Microbiol 71: 2154-2157.
687 Steele, J.A., Countway, P.D., Xia, L., Vigil, P.D., Beman, J.M., Kim, D.Y. et al. (2011)
688 Marine bacterial, archaeal and protistan association networks reveal ecological linkages.
689 ISME J 5: 1414.
690 Stoeck, T., Bass, D., Nebel, M., Christen, R., Jones, M.D., BREINER, H.W., and Richards,
691 T.A. (2010) Multiple marker parallel tag environmental DNA sequencing reveals a highly
692 complex eukaryotic community in marine anoxic water. Mol Ecol 19: 21-31.
693 Teeling, H., Fuchs, B.M., Becher, D., Klockow, C., Gardebrecht, A., Bennke, C.M. et al.
694 (2012) Substrate-controlled succession of marine bacterioplankton populations induced by a
695 phytoplankton bloom. Science 336: 608-611.
696 Teeling, H., Fuchs, B.M., Bennke, C.M., Krueger, K., Chafee, M., Kappelmann, L. et al.
697 (2016) Recurring patterns in bacterioplankton dynamics during coastal spring algae blooms.
698 Elife 5: e11888.
699 Thyssen, M., Grégori, G.J., Grisoni, J.-M., Pedrotti, M.L., Mousseau, L., Artigas, L.F. et al.
700 (2014) Onset of the spring bloom in the northwestern Mediterranean Sea: influence of
701 environmental pulse events on the in situ hourly-scale dynamics of the phytoplankton
702 community structure. Front Microbiol 5: 387.
703 Tinta, T., Vojvoda, J., Mozetič, P., Talaber, I., Vodopivec, M., Malfatti, F., and Turk, V.
704 (2015) Bacterial community shift is induced by dynamic environmental parameters in a
705 changing coastal ecosystem (northern A driatic, northeastern M editerranean S ea)–a 2-year
706 time-series study. Environ Microbiol 17: 3581-3596.
707 Treusch, A.H., Vergin, K.L., Finlay, L.A., Donatz, M.G., Burton, R.M., Carlson, C.A., and
708 Giovannoni, S.J. (2009) Seasonality and vertical structure of microbial communities in an
709 ocean gyre. ISME J.
710 Vellend, M. (2010) Conceptual synthesis in community ecology. Q Rev Biol 85: 183-206.

Wang, Q., Garrity, G.M., Tiedje, J.M., and Cole, J.R. (2007) Naive bayesian classifier for rapid assignment of rRNA sequences into the new bacterial taxonomy. Appl Environ Microbiol 73: 5261-5267.

Ward, C.S., Yung, C.-M., Davis, K.M., Blinebry, S.K., Williams, T.C., Johnson, Z.I., and Hunt, D.E. (2017) Annual community patterns are driven by seasonal switching between closely related marine bacteria. ISME J 11: 1412.

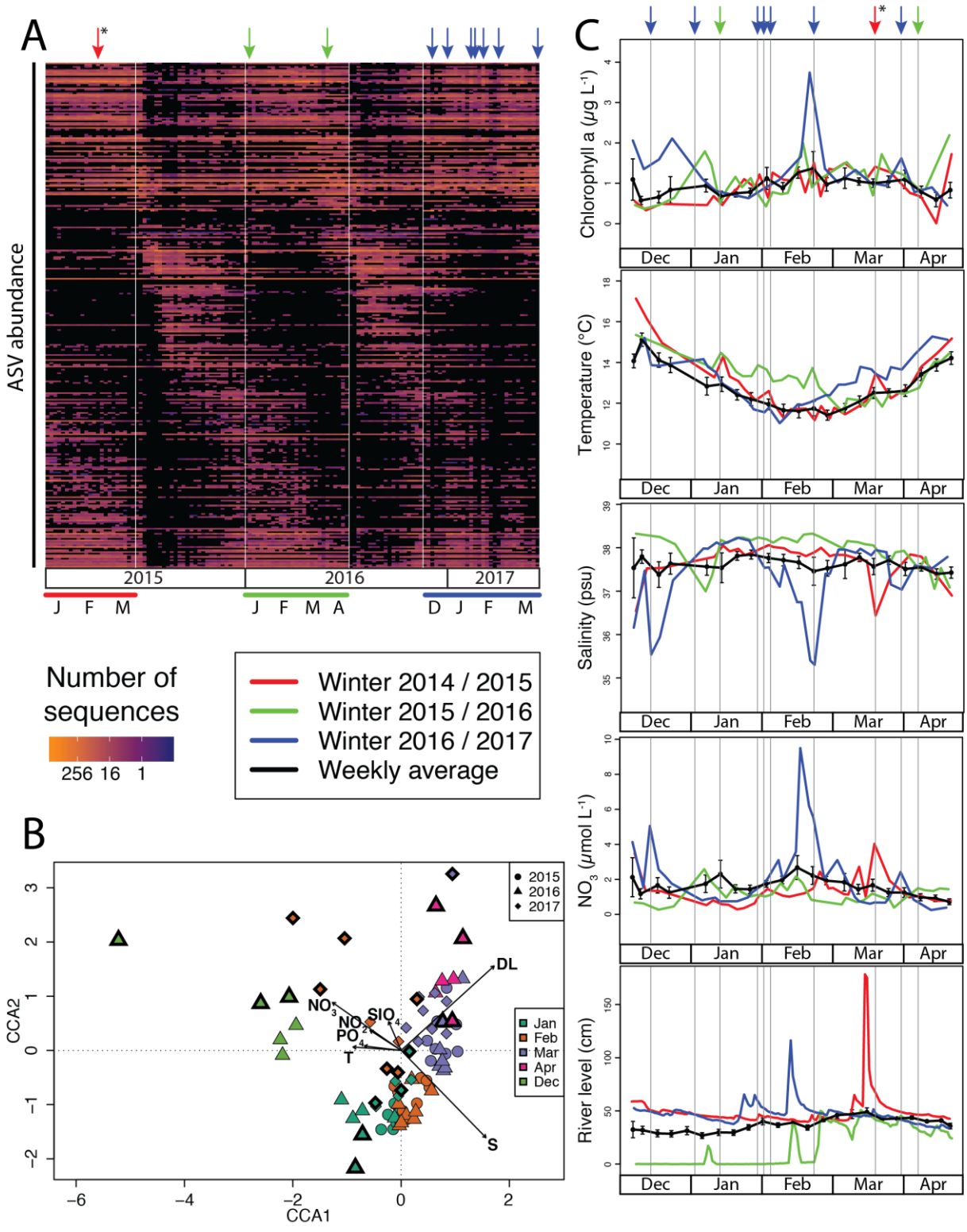
A
ASV abundance
2015
2016
2017
J F M
J F M A
D J F M
Number of sequences
256 16 1
Winter 2014 / 2015
Winter 2015 / 2016
Winter 2016 / 2017
Weekly average
B
CCA1
CCA2
2015
2016
2017
Jan
Feb
Mar
Apr
Dec
DL
S
T
C
Chlorophyll a (µg L-1)
Temperature (°C)
Salinity (psu)
NO3 (µmol L-1)
River level (cm)
Dec
Jan
Feb
Mar
Apr

Fig. 1

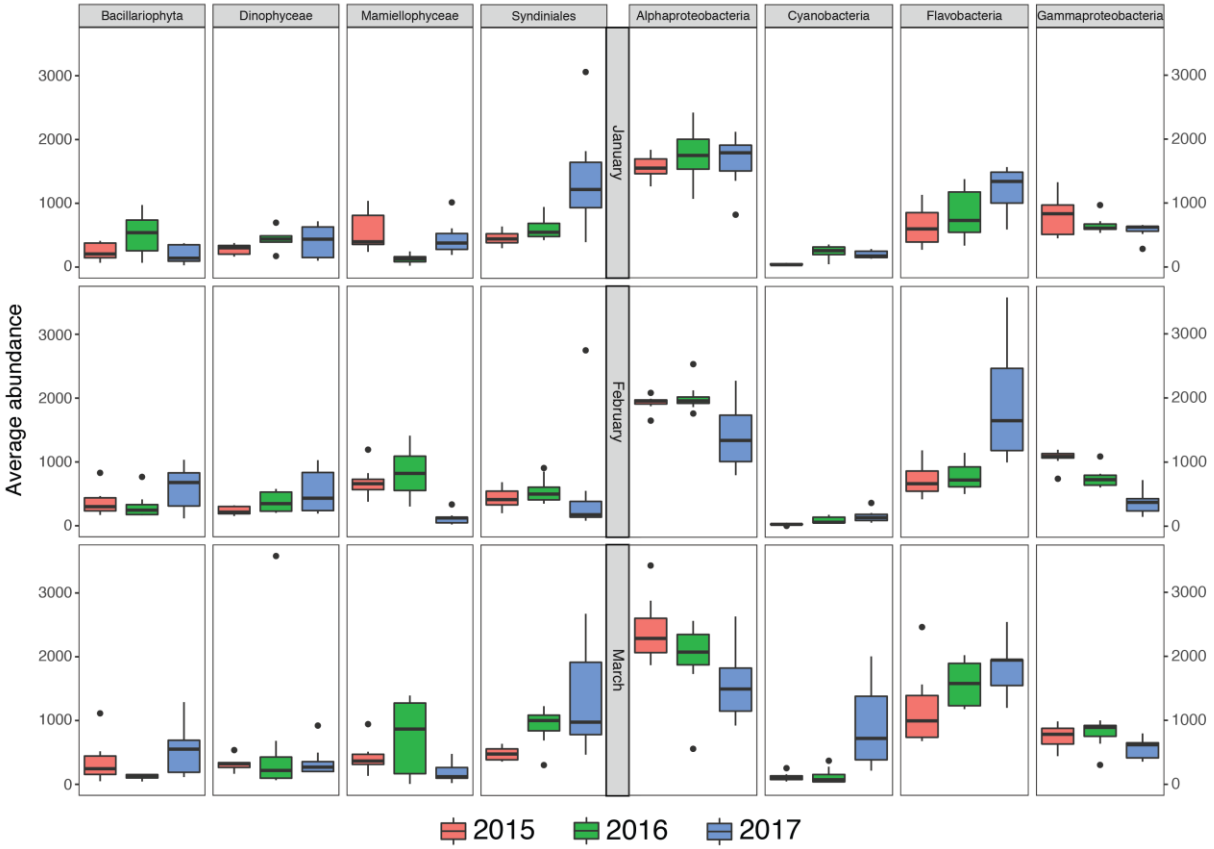
Bacillariophyta
Dinophyceae
Mamiellophyceae
Syndiniales
Alphaproteobacteria
Cyanobacteria
Flavobacteria
Gammaproteobacteria
January
February
March
Average abundance
0
1000
2000
3000
2015
2016
2017

Fig 2

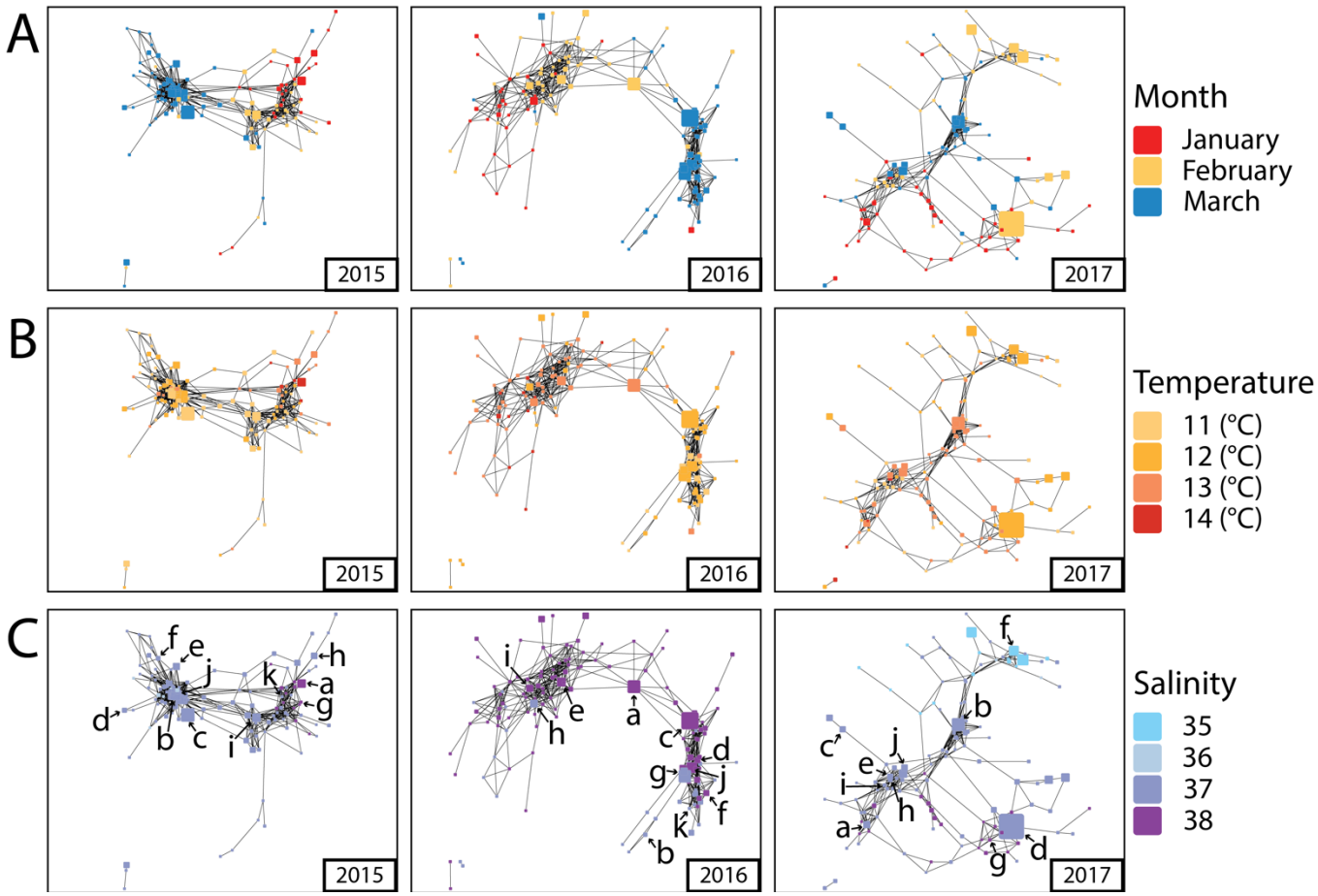
A
B
C
2015
2016
2017
Month
January
February
March
Temperature
11 (°C)
12 (°C)
13 (°C)
14 (°C)
Salinity
35
36
37
38

Fig 3

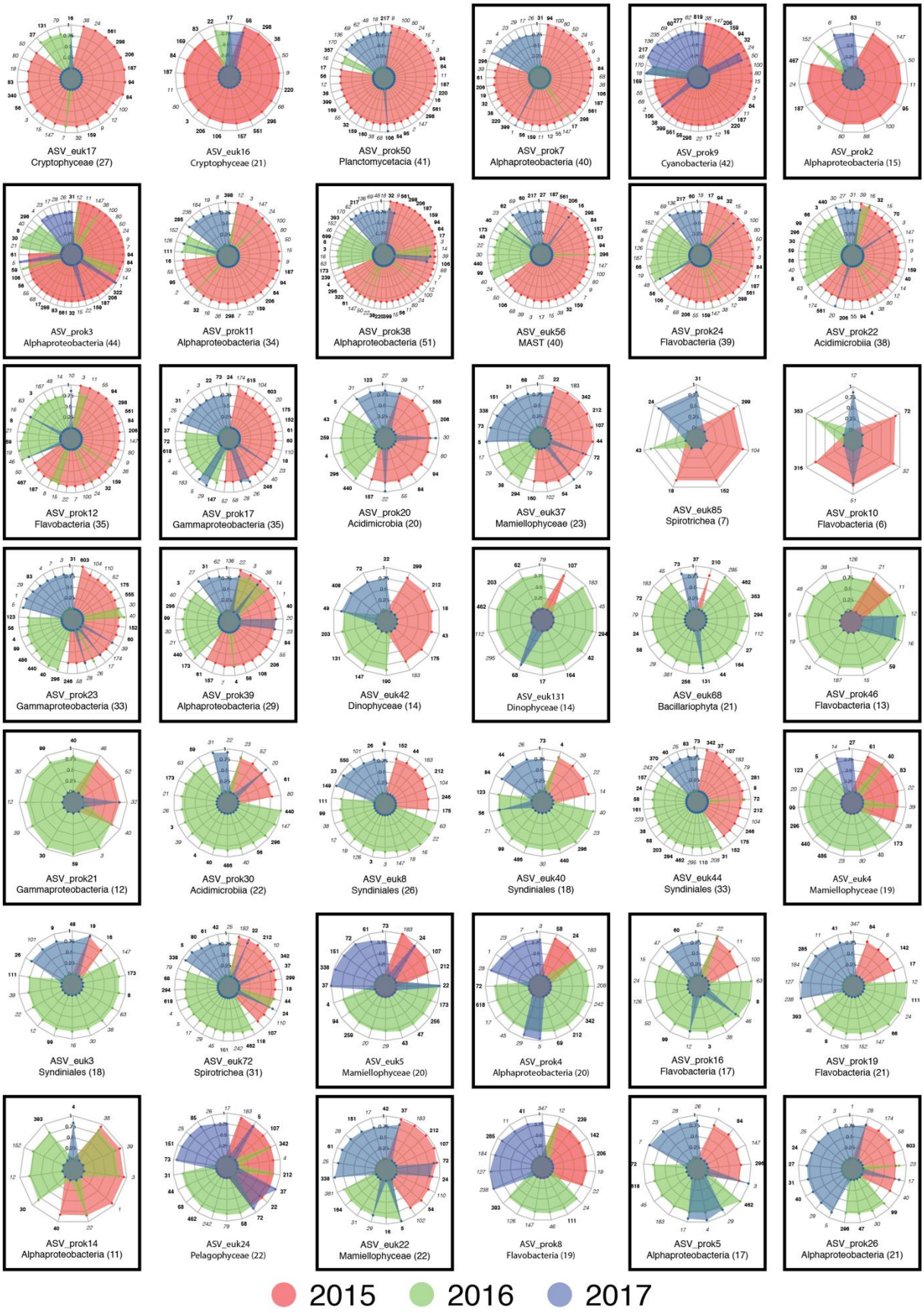
ASV_euk17
Cryptophyceae (27)
ASV_euk16
Cryptophyceae (21)
ASV_prok50
Planctomycetacia (41)
ASV_prok7
Alphaproteobacteria (40)
ASV_prok9
Cyanobacteria (42)
ASV_prok2
Alphaproteobacteria (15)
ASV_prok3
Alphaproteobacteria (44)
ASV_prok11
Alphaproteobacteria (34)
ASV_prok38
Alphaproteobacteria (51)
ASV_euk56
MAST (40)
ASV_prok24
Flavobacteria (39)
ASV_prok22
Acidimicrobiia (38)
ASV_prok12
Flavobacteria (35)
ASV_prok17
Gammaproteobacteria (35)
ASV_prok20
Acidimicrobia (20)
ASV_euk37
Mamiellophyceae (23)
ASV_euk85
Spirotrichea (7)
ASV_prok10
Flavobacteria (6)
ASV_prok23
Gammaproteobacteria (33)
ASV_prok39
Alphaproteobacteria (29)
ASV_euk42
Dinophyceae (14)
ASV_euk131
Dinophyceae (14)
ASV_euk68
Bacillariophyta (21)
ASV_prok46
Flavobacteria (13)
ASV_prok21
Gammaproteobacteria (12)
ASV_prok30
Acidimicrobiia (22)
ASV_euk8
Syndiniales (26)
ASV_euk40
Syndiniales (18)
ASV_euk44
Syndiniales (33)
ASV_euk4
Mamiellophyceae (19)
ASV_euk3
Syndiniales (18)
ASV_euk72
Spirotrichea (31)
ASV_euk5
Mamiellophyceae (20)
ASV_prok4
Alphaproteobacteria (20)
ASV_prok16
Flavobacteria (17)
ASV_prok19
Flavobacteria (21)
ASV_prok14
Alphaproteobacteria (11)
ASV_euk24
Pelagophyceae (22)
ASV_euk22
Mamiellophyceae (22)
ASV_prok8
Flavobacteria (19)
ASV_prok5
Alphaproteobacteria (17)
ASV_prok26
Alphaproteobacteria (21)
2015
2016
2017

Fig 4

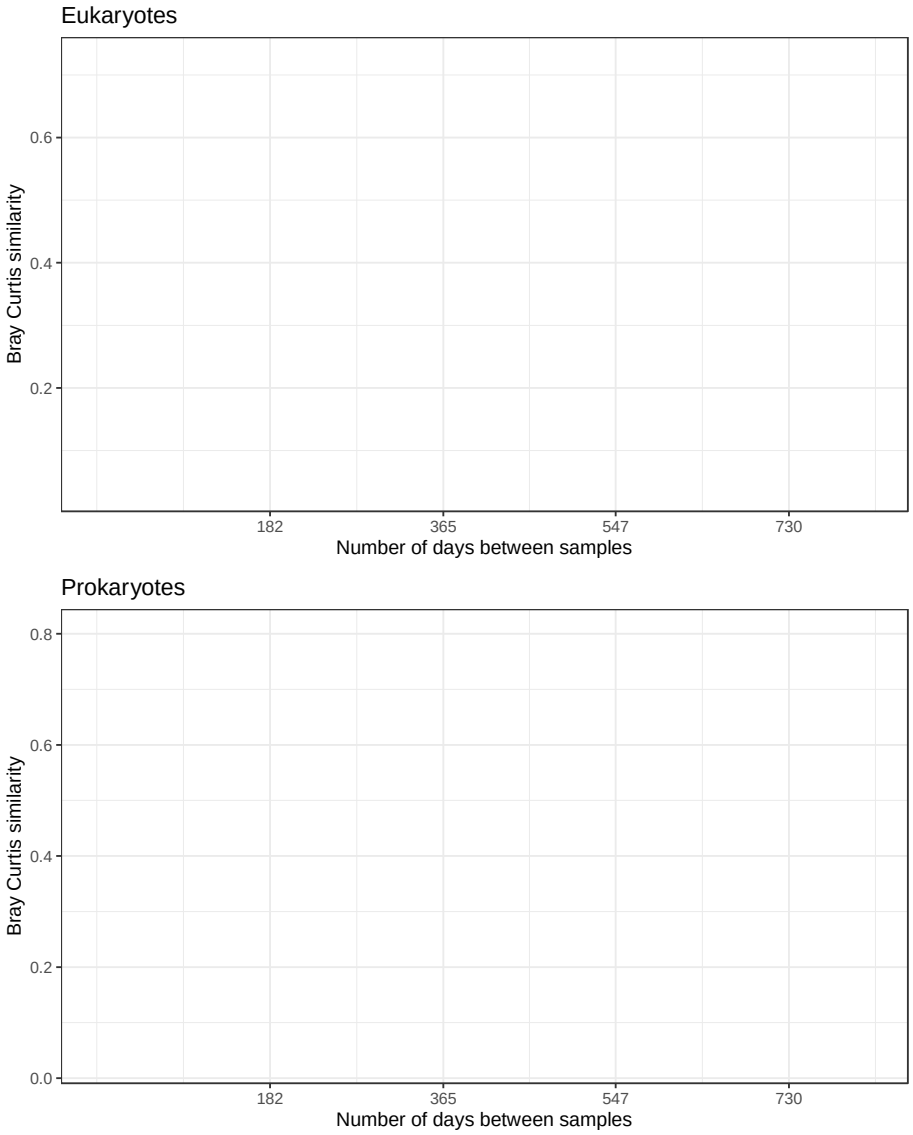

Supplementary Fig. 1

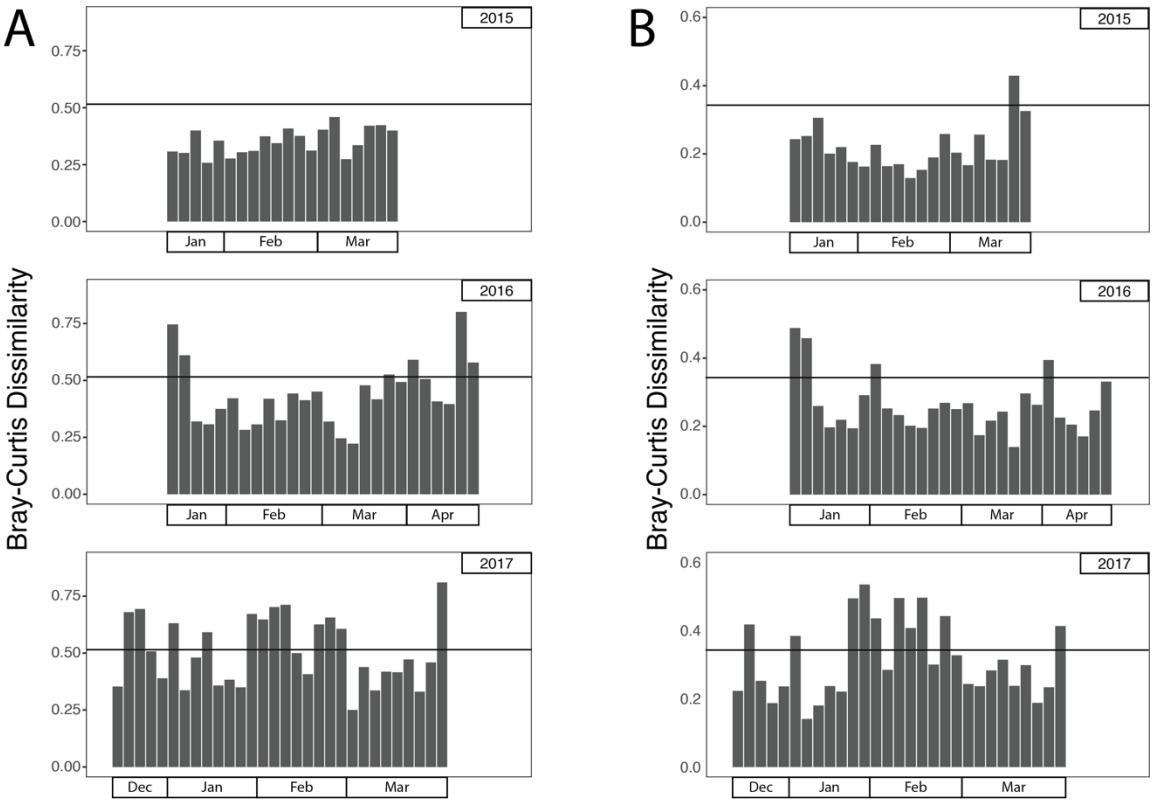

Supplementary Fig. 2

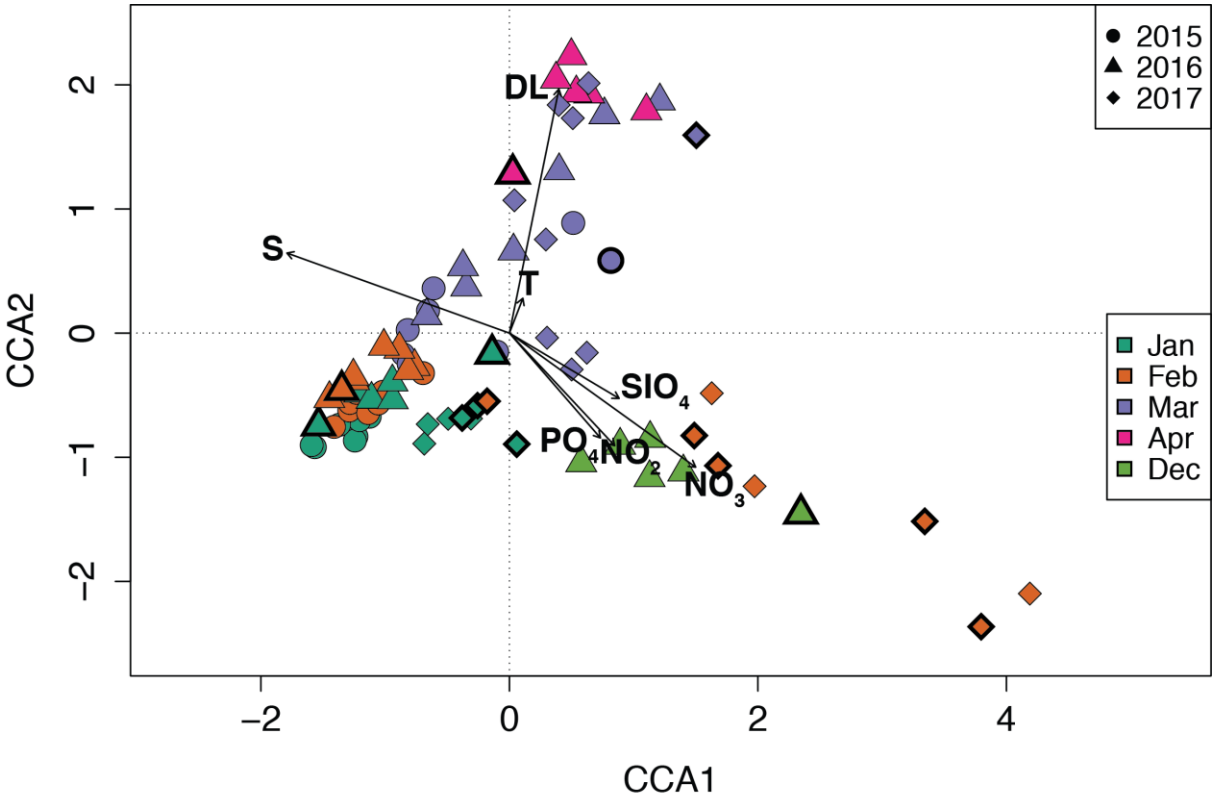

Supplementary Fig. 3

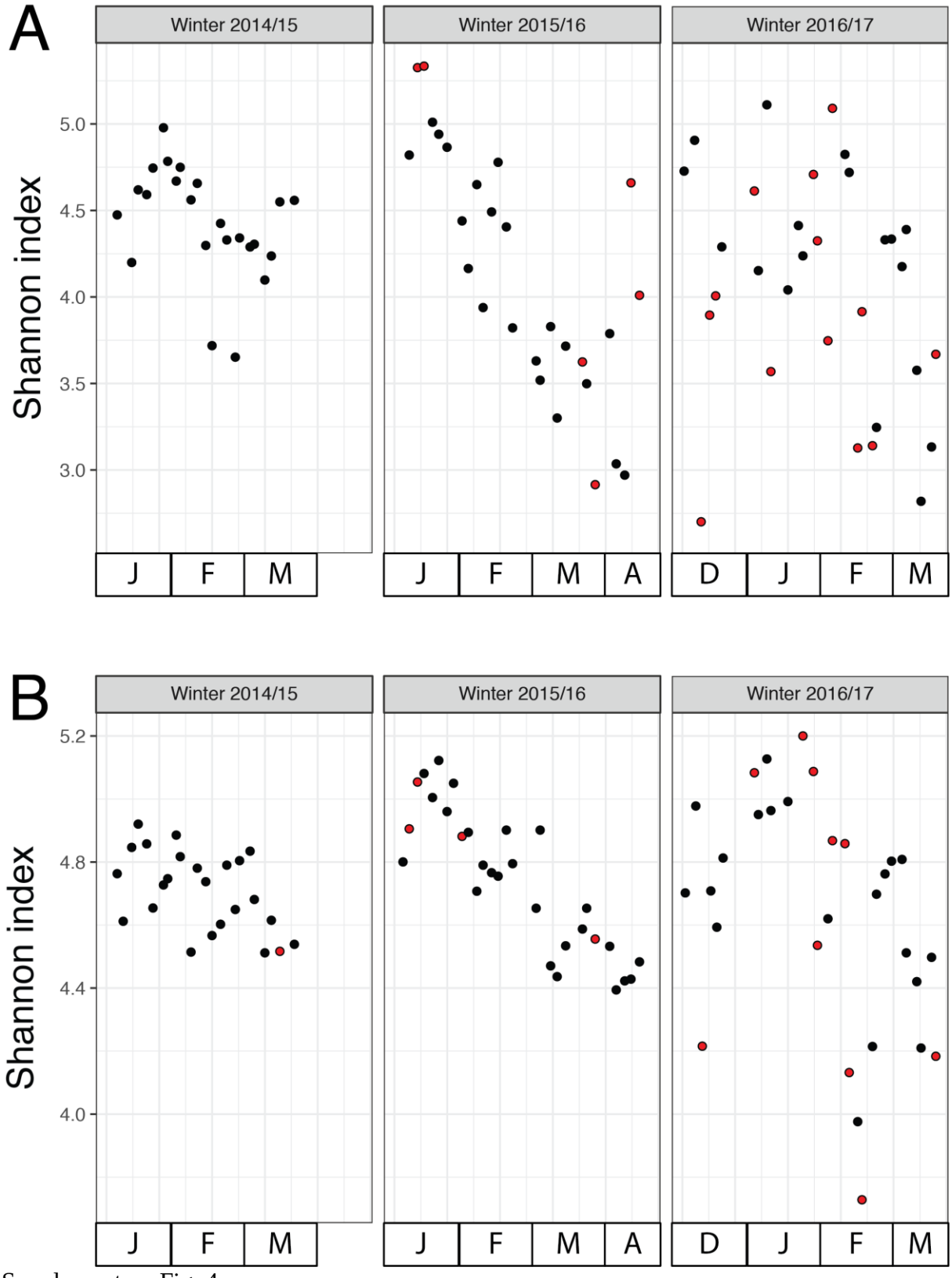

Supplementary Fig. 4

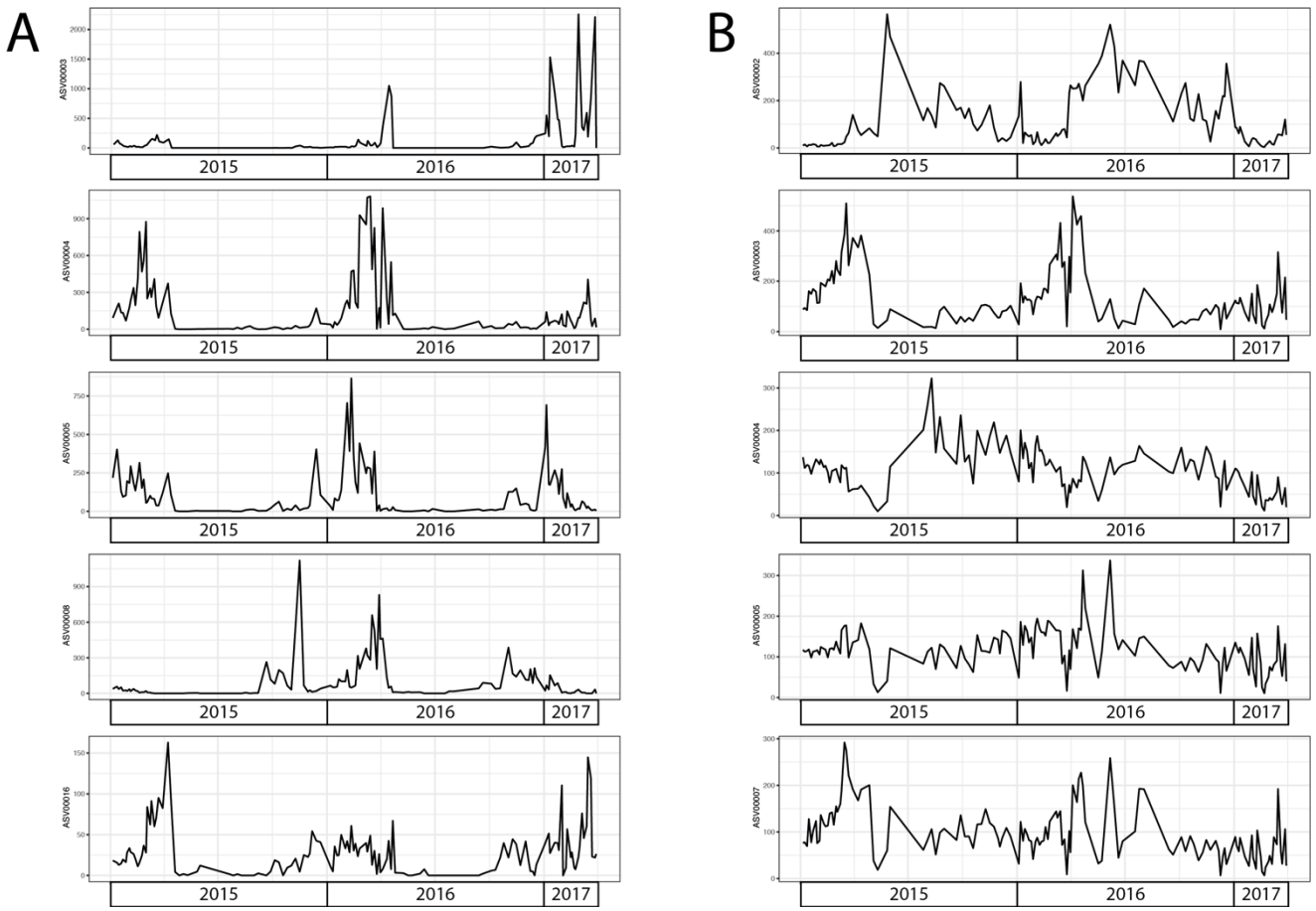

Supplementary Fig. 5

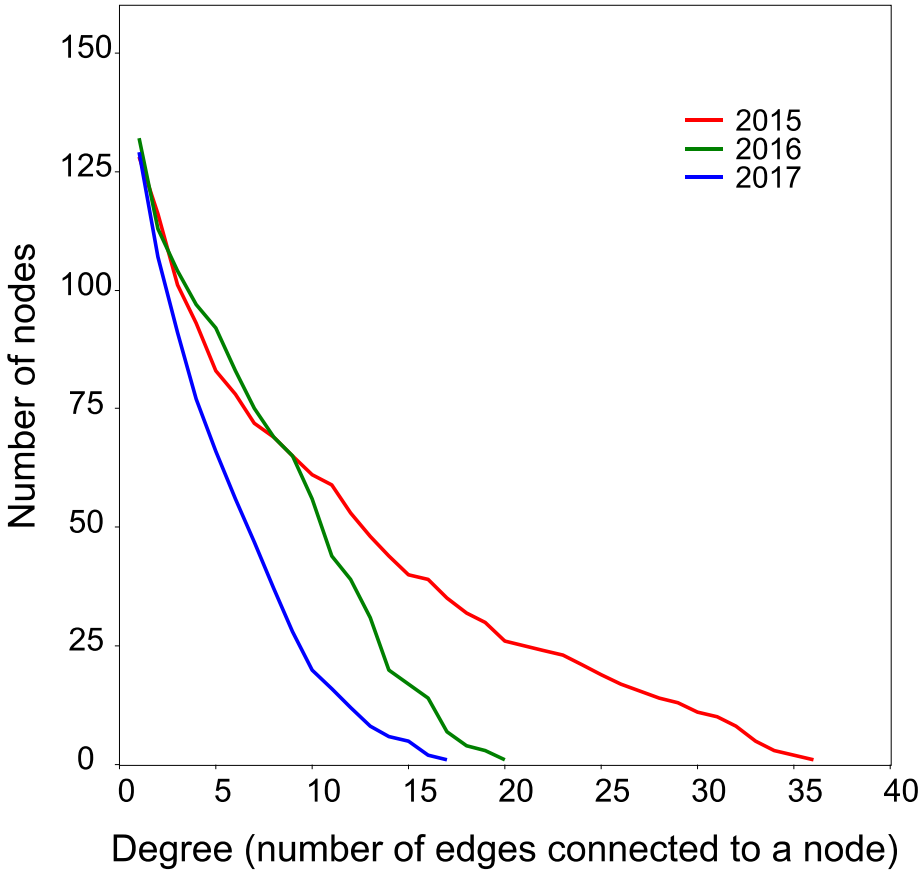

Supplementary Fig. 6

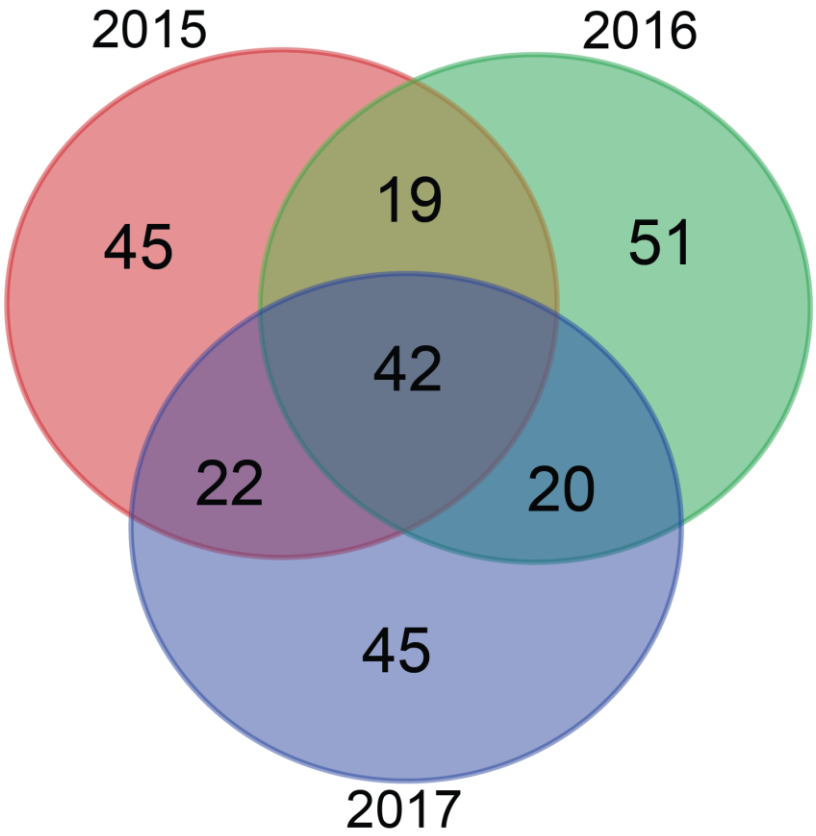

Supplementary Fig. 7